# KINETICS OF FORMATION AND THERMAL AND MECHANICAL PROPERTIES OF CHAR OBTAINED BY ULTRA-HIGH TEMPERATURE PYROLYSIS OF POLYETHYLENE VIA MOLECULAR DYNAMICS SIMULATIONS

Maxim A. Makeev, John W. Lawson, Deepak Srivastava

NASA Ames Research Center, Mail Stop 229-1,
Moffett Field, CA 94035 USA

Keywords: pyrolytic char, atomistic simulations, elastic properties, thermal conductivity

## Abstract

We report results of a molecular dynamics simulation study of the high-temperature pyrolysis of polyethylene (PE) and the mechanical and thermal properties of the resultant carbonaceous char. The microstructure of pyrolyzed PE samples was monitored during the simulation. Mechanical properties of the resultant char were studied for char samples with varied microstructure (average coordination number and ring-size distributions) to establish structure-property relationships between mechanical (thermal) response properties and microstructure. We found that this relationship can be established based upon the random network theory of amorphous media, if additional topological constraints due to rings are taken into account. Thermal conductivity of pyrolytic char is investigated for samples with different microstructures for a wide range of temperatures. Similar to the mechanical response, the thermal response properties are correlated to microstructure. It is shown that the behavior of the thermal conductivity can be well described by Einstein's heat transfer theory, if microstructure effecs are taken into account.

## Introduction

The process of phase transformation under ultra-high temperature treatment is of interest from both fundamental science and technology perspectives. Among many others realizations of this phenomenon, pyrolysis of polymeric materials has been extensively investigated to understand the kinetic and microstructural aspects of char formation [1,2,3]. For example, the chemical processes involved in thermal decomposition of polyethylene have been investigated in [1,2]. Reverse Monte Carlo modeling of char microstructure, performed on industrial char samples, has been reported in Ref. [3]. It was found that char contains buckled graphene sheets. Additionally, ultra-high temperature pyrolysis experiments of carbon nanotube-filled polymer-matrix composites have recently been performed and structures of the resultant char samples have been investigated. These studies have been performed for polymethyl methacrylate/carbon nanotube [4] and polypropylene/carbon nanotube [5,6] nanocomposites. For both materials, the integral char yield was found to increase as compared with pristine polymer systems. In general, it is understood by now that the process of pyrolysis of macromolecular systems (pristine and composites) is a complex phenomenon, dependent on various aspects of initial polymer-sample microstructure and pyrolysis conditions. The resultant microstructure of char samples has also been the focus of investigations in the past. One important aspect of Ref. [3] should particularly be emphasized. In that work, the fact that char can include structural units of buckled graphitic sheets was particularly importance for microstructure studies, as the observed picture clearly differed from random networks which had been previously shown to provide an adequate

| 1. REPORT DATE **FEB 2009** | 2. REPORT TYPE | 3. DATES COVERED **00-00-2009 to 00-00-2009** |
|---|---|---|

| 4. TITLE AND SUBTITLE | 5a. CONTRACT NUMBER |
|---|---|
| **Kinetics of Formation and Thermal and Mechanical Properties of Char Obtained by Ultra-High Temperature Pyrolysis of Polyethylene via Molecular Dynamics Simulations** | 5b. GRANT NUMBER |
| | 5c. PROGRAM ELEMENT NUMBER |

| 6. AUTHOR(S) | 5d. PROJECT NUMBER |
|---|---|
| | 5e. TASK NUMBER |
| | 5f. WORK UNIT NUMBER |

| 7. PERFORMING ORGANIZATION NAME(S) AND ADDRESS(ES) **NASA Ames Research Center,Mail Stop 229-1,,Moffett Field,CA,94035** | 8. PERFORMING ORGANIZATION REPORT NUMBER |
|---|---|

| 9. SPONSORING/MONITORING AGENCY NAME(S) AND ADDRESS(ES) | 10. SPONSOR/MONITOR'S ACRONYM(S) |
|---|---|
| | 11. SPONSOR/MONITOR'S REPORT NUMBER(S) |

12. DISTRIBUTION/AVAILABILITY STATEMENT
**Approved for public release; distribution unlimited**

13. SUPPLEMENTARY NOTES
**See also ADM002300. Presented at the Minerals, Metals and Materials Annual Meeting and Exhibition (138th)(TMS 2009) Held in San Francisco, California on February 15-19, 2009. Sponsored in part by the Navy.**

14. ABSTRACT
**We report results of a molecular dynamics simulation study of the high-temperature pyrolysis of polyethylene (PE) and the mechanical and thermal properties of the resultant carbonaceous char. The microstructure of pyrolyzed PE samples was monitored during the simulation. Mechanical properties of the resultant char were studied for char samples with varied microstructure (average coordination number and ring-size distributions) to establish structure-property relationships between mechanical (thermal) response properties and microstructure. We found that this relationship can be established based upon the random network theory of amorphous media, if additional topological constraints due to rings are taken into account. Thermal conductivity of pyrolytic char is investigated for samples with different microstructures for a wide range of temperatures. Similar to the mechanical response, the thermal response properties are correlated to microstructure. It is shown that the behavior of the thermal conductivity can be well described by Einstein?s heat transfer theory, if microstructure effecs are taken into account.**

15. SUBJECT TERMS

| 16. SECURITY CLASSIFICATION OF: | | | 17. LIMITATION OF ABSTRACT | 18. NUMBER OF PAGES | 19a. NAME OF RESPONSIBLE PERSON |
|---|---|---|---|---|---|
| a. REPORT **unclassified** | b. ABSTRACT **unclassified** | c. THIS PAGE **unclassified** | **Same as Report (SAR)** | **8** | |

description for a wide range of amorphous solids [7,8]. In light of the above, finding structure-property relationships for disordered systems with complex microstructures is of great importance.

In the present work, we study the mechanical and thermal properties of char, obtained by high-temperature pyrolysis of a model PE sample, with the main emphasis on structure-property relationships. The molten-phase carbonaceous char was obtained by high-temperature pyrolysis using methodology previously described in Ref. [9]. In brief, a pyrolytic molecular dynamics simulation approach was devised and used to study the process of polyethylene charring. The approach includes the kinetics of temperature-mediated hydrogen removal from the system and high-temperature relaxation of the carbonaceous char. For more details of the approach, the reader is referred to Ref. [9]. Moreover, we have recently performed more detailed simulation studies of the pyrolytic charring process, with particular emphasis on the kinetics of dehydrogenation and the resultant amorphous carbon structure evolution under different conditions. The major focus of the present study is the basics of *the kinetics of char formation and the mechanical and thermal* properties of solid-state char samples. To obtain amorphous char samples with different microstructures, the high-temperature molten-state char sample was quenched at different cooling rates and/or relaxation times. A total of five carbonaceous char samples (differing in microstructure) was obtained and investigated for mechanical and thermal response properties.

## Kinetics of pyrolysis

An initial simulation system consisted of amorphous PE cell with dimensions along the *x*- and *y*-axis equal to 22 Å and along the *z*-axis equal to 87 Å. Periodic boundary conditions were applied to the system in all three directions. The system contained 40 PE chains, with the total number of atoms equal to 4880, out of which 1600 were carbon atoms and 3280 were hydrogen atoms. The Brenner reactive, bond-order potential (REBO) was used to describe interactions between hydrogen and carbon atoms [10]. In the past, this potential has been successfully used to model dynamic breaking and formation of chemical bonds under broad range of conditions.

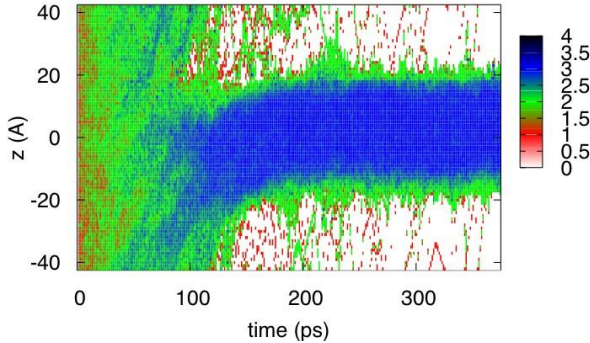

Figure 1. The color-coded map shows dynamical evolution of coordination numbers of carbon atoms in PE during pyrolysis at T=5000 K. The nucleation of char and the collapse of the original structure are illustrated by corresponding changes in the average coordination numbers.
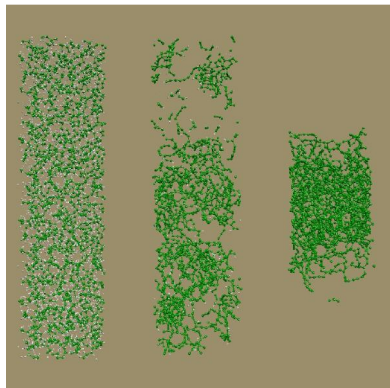
Figure 2. The collapse of dehydrogenated carbon network during cooling: a) snapshot of the initial simulation system; b) snapshot of the simulation system after $t$ =90 ps; c) the collapsed carbon network visualized at $t$ = 200 ps.

The dynamics of char formation is realized through C-H bond breaking and the removal of free hydrogen atoms from the system. A proper scheme for removal of hydrogen atoms is essential for formation of a cross-linked carbon networks and collapse of the dehydrogenated system into a dense (highly coordinated) carbonaceous char structure. In real polymer systems, free hydrogen atoms will diffuse out of the system at elevated temperatures through a free surface or some other interface. To accelerate the process of hydrogen removal (which is essential to simulate charring within MD time-scales), hydrogen atoms were removed from the system after they became free of the polymer during the course of dynamics. A hydrogen atom was considered free if it was outside the range of the Brenner potential. In Fig. 1, a color-coded map showing the dynamical evolution of the average carbon coordination number is presented for the PE sample pyrolysed at T=5000 K. The simulation cell was divided into slices of thickness ≈1 Å along the $z$-direction (parallel to the $x$-$y$ plane). The average coordination numbers for C atoms were computed in each bin and plotted as a function of time. In the figure, the average coordination of 1 is depicted in red color, while an average coordination of 2, 3, and 4 is shown in green, purple, and blue, respectively. As can be observed in the figure, at $t$ = 0, the average coordination numbers are either one or two, thus being consistent with the original PE microstructure. At larger simulation times, the average coordination numbers changed from a mixture of one and two (red and green) to pockets of threefold coordination around $t$ = 50 ps. The appearance of threefold-coordination regions indicates the formation of graphitic cross-links in the structure. These cross-links act as nucleation centers, which grow and then merge forming larger, more highly coordinated structures. The interiors of these regions have mixed threefold and fourfold coordination numbers, indicating smaller, diamond-like structures in the core. By $t$ = 80 ps, much of the simulation cell has mixed threefold or fourfold coordination, but the structure is still distributed along the entire cell. By $t$ = 100 ps, however, the inner core of the threefold coordinated regions starts to nucleate fourfold regions and the rest of the structure starts to othe final evolved structure, thus, has highest coordination values three or four in the interior of the char with smaller values of 3 and 2 observed toward the surface. Since the system has collapsed

to less than half the original volume of the simulation cell, the density of the carbon structure has increased proportionally to an approximate value of 1.67 g/cm$^3$ (initial density being 0.89 g/cm$^3$). One can also observe that dynamical processes continue after the system has collapsed, with small carbon fragments continuing to be ejected and absorbed.

### Char properties: Young's modulus

The mechanical response properties of carbonaceous char samples were studied for five samples with different microstructural characteristics (*i.e.*, average coordination numbers and ring statistics). To investigate the mechanical response properties, dynamical loadings were performed on each sample by rescaling the coordinates by a factor of 0.001 along the sample's largest dimension (*z*-axis). The applied tensile (or compressive) load corresponds to strain value of $\approx$0.1%. To model the adiabatic loading, the char samples after each loading step were first relaxed at elevated temperatures for no less than 5000 MD steps and, subsequently, were cooled down to T=5 K. The total energy of the loaded system, $E_s$, was computed after each loading step. The elastic energy due to tensile (or compressive) loading was computed as $E_s$-$E_0$, where $E_0$ is the total energy of the unloaded sample. The step-wise loading was continued until the strain reached the value of $\approx$15%. The strain energy was found to be a quadratic function of the applied strain for all considered samples. The Young's modulus was obtained by fitting a quadratic form to the simulation data.

To analyze the obtained data, we invoked the *random network* theory of disordered (glassy) solids. The idea of representing disordered solids as random networks was introduced by Zachariansen in as early as 1932, based upon X-ray diffraction experiments performed on SiO$_4$ glasses. Subsequently, this concept has been developed into a rigorous mathematical theory of network elasticity (by Phillips [7] and Thorpe [8]). In the following, we employ the framework of theory of random network continuous deformation to interpret our simulation results. First, let us briefly overview the basics of the theory [7,8]. We consider a random network of bonds connecting nodes, where each node corresponds to an atom in glassy material. The major quantity of interest is the average coordination number, $<r>$, defined as $<r> = \sum r n_r / \sum n_r$, where $r$ is the number of bonds and $n_r$ is the *number* of atoms having $r$ bonds. Dependent on network connectivity, a random network can be considered as a polymeric glass or amorphous solid. The transition between these two regimes occurs at $<r> = r_p = 2.4$ [8]. These classification derives from percolation theory and are based on considering percolation of floppy (soft) and rigid regions, with amorphous solids corresponding to a network connectivity above the threshold, *i.e.*, $<r>$ being greater than 2.4. It should be noted that the above holds for random networks without rings. As we show below, ring corrections can introduce considerable modifications to the above framework. To analyze our simulation data for the microstructure effects on the elastic response, we use the following expression for the Young's modulus dependence on $<r>$:

$$Y = Y_0 \left( \frac{<r> - 2.4}{r_0 - 2.4} \right)^{1.5} , \qquad (1)$$

where $Y_0$ is the Young's modulus of the network with connectivity $r_0$ and $r_p$ is the threshold value for the percolation transition, defined by microstructural properties of the network [11]. In our analysis, $r_0$ corresponds to 100% sp$^3$ *a*-C network, *i.e.*, $r_0 = 4$, and $Y_0$ (=823 GPa) is the Young's modulus of the 100% sp$^3$ amorphous carbon.
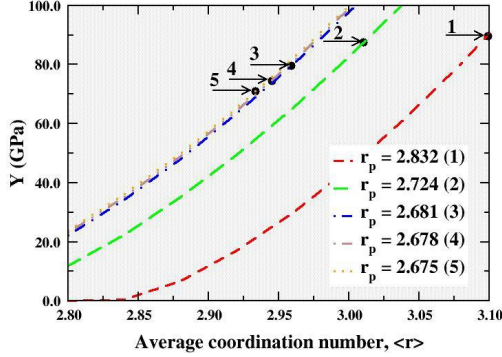
Figure 3. Young's modulus of five carbonaceous char samples is shown as a function of the average coordination number (solid circles). The lines represent the dependence of the Young's modulus on <r>, plotted for different values of $r_p$.

As can be observed in the figure, the dependence significantly differs from results reported on random networks. Indeed, it is clear, that a super-linear dependence cannot provide an adequate description of the observed behavior. Consequently, while elastic responses of a purely random network are known to demonstrate a ~ $<r>^{1.5}$ dependence with average coordination number, our results differ significantly from this type of behavior. One of the key parameters of the theory of random networks is the percolation threshold $r_p$, which separates the polymeric glass and amorphous glass phases. As the simulation results demonstrate, our char samples are not pure random networks, as they contain a non-zero density of rings of sizes varied from 3 to 8. The effects of rings have been previously considered in Ref. [8]. It was shown that the presence of rings introduces a correction to the percolation threshold in the form $r_p = 2.4 + \delta$, where $\delta$ is defined by densities of the rings in the system. Following the approach developed in Ref. [8], we found that the correction factor $\delta$ in our char samples varies from ≈0.275 to 0.430. Consequently, the dependence of the elastic modulus on the coordination number in our samples should include the variance in the parameter $r_p$. The computed values of corrections (shown in Fig. 3) are in good agreement with the values for this parameter, obtained by fits to the simulation data. Consequently, the elastic properties of amorphous carbon are defined by average coordination number and a ring-size distribution. The observed ring structures introduce a significant change in the mechanical response properties of char as compared with *purely random network glasses*.

### Char properties: Thermal conductivity

The thermal conductivity of char samples was investigated using the direct method for thermal conductivity measurement in molecular dynamics. This scheme is based upon the Fourier law of heat conduction [12]. The adopted scheme is as follows. The simulation cell was divided along the z-axis into 100 equal-size units. Two slabs, located at $L_z/4$ and $-L_z/4$ with respect to the center of the system, are used as a heat source and a heat sink, respectively. The velocity of each atom, residing in these slabs, was rescaled at each MD step to increase/decrease the kinetic energy by a fixed value $\pm\Delta\varepsilon$, such that the total energy of the system is conserved. The procedure

is continued until the system is equilibrated, with the temperature gradient reaching a constant value. The thermal conductivity is computed using the following expression

$$J_z = -\lambda \frac{\partial T}{\partial z} \quad ,$$

(2)

where $\lambda$ is the thermal conductivity and $J_z = \Delta\varepsilon/(2L_xL_y\Delta t)$ is the heat flux. The temperature dependence of the thermal conductivity of our char sample with largest coordination number ($<r> = 3.10$) is presented in Fig. 4. As can be observed in the figure, the thermal conductivity gradually increases with temperature in the studied range of temperatures, with behavior at highly elevated temperatures indicating near saturation, compared with the fast growth in the low and moderate temperature regimes. This behavior can be understood in terms of incoherent atomic vibrations. As the temperature increases, the mean free path of such vibrations decreases and, at very high temperatures, becomes comparable with an average inter-atomic distance. The saturation value of the thermal conductivity can be estimated as $\lambda = 1/3\ C_v v\ a$, where $C_v$ is the specific heat, $v$ is the velocity of sound, and $a$ is the average interatomic distance. It should be noted, however, that, in the limit of very high temperatures, the behavior of the thermal conductivity can be affected by enhanced phonon-phonon scattering and temperature-activated microstructural changes. These effects can lead to decreases with temperature of the thermal conductivity in high temperature regimes. We observed structural relaxation in systems heated above $\approx$600 K.

To provide an analytical description of the thermal conductivity, we use Einstein's theory of heat transport [13]. In the past, this theory has been successfully applied to interpret experimental data on the thermal conductivity of disordered solids [13] and amorphous carbon thin films [14].



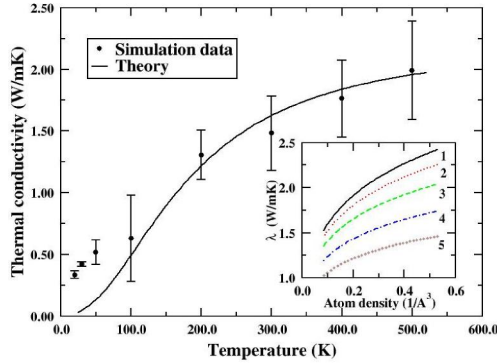Figure 4.  The thermal conductivity versus temperature is shown for char sample with $<r> = 3.10$. Shown in the inset are the behaviors of the thermal conductivity with atomic density (measured in $1/\text{Å}^3$) for different values of Young's modulus (decreasing from 1 to 5).

The approach is based upon the assumption of diffusive heat transfer by incoherent atomic vibrations. The heat diffusion takes place between Einstein oscillators on a time scale of half of the period of vibration. Within this approach, the minimum value of the thermal conductivity can be estimated as

$$\lambda_{\min} = \left(\frac{\pi}{6}\right)^{1/3} k_B n^{2/3} \sum_{i=1,2,3} v_i \left(\frac{T}{\Theta_i}\right)^2 \int_o^{\Theta_i/T} \frac{x^3 e^x}{(e^x - 1)^2} dx \quad . \tag{3}$$

In the above equation, index $i = 1,2,3$ marks two transverse and one longitudinal sound modes, traveling with speeds $v_i$, $\Theta_i = v_i (h/k_B) (6\pi^2 n)^{1/3}$ ($i=1,2,3$) are the cut-off frequencies of these three modes (expressed in Kelvin), and $n$ is the number density of carbon atoms (expressed in $1/\text{Å}^3$). The analytical dependence of the thermal conductivity as a function of temperature, obtained using Eq. (3), is shown in Fig. 4 as a solid line. As can be observed in the figure, the theoretical approach provides an appropriate qualitative description of the behavior by capturing the major trends of the behavior. This is particularly true for the behavior at elevated temperatures (for temperatures exceeding 100 K). In the low temperature regime, deviations from the model prediction take place. These deviations are due to substantial differences between classical MD temperatures and quantum temperatures. In other words, in the low-temperature regime, quantum corrections become significant and should be taken into account to achieve a better description of the thermal conductivity. The analytical form Eq. (3) can be used to predict the thermal conductivity dependence for samples differing in microstructure. In the inset to Fig. 4, we show the thermal conductivity dependence on atomic density for samples with different elastic properties. We used Eq. (1) to relate the microstructure to elastic modulus. Knowing the elastic properties of samples, it is straightforward to obtain the corresponding velocities of sound. Note that the obtained ranges of thermal conductivity variations are in good agreement with previously reported experimental data [14].

### Summary and conclusions

In summary, MD simulations with Brenner bond-order reactive potential have been employed to study mechanical and thermal response properties of carbonaceous char samples with differing microstructure. Hot char samples were prepared using previously developed pyrolytic MD method as applied to polyethylene. A set of char samples with varied microstructure has been generated using different annealing regimes applied to the hot char. We used the results on microstructure to provide an interpretation of thermal and mechanical behavior based upon variations in char microstructure. First, we computed the mechanical responses of five char samples (differing in microstructure) and interpreted the obtained results in terms of random network theory of amorphous solids taking into account corrections due to rings. The results allowed us to predict the mechanical response as a function of microstructural properties. Using the direct method for thermal conductivity measurement in molecular dynamics, we investigated the thermal conductivity of char samples. We found that the thermal conductivity can be well described by the "incoherent vibrations model", with all the essential features of its behavior captured within the framework this model. This includes the temperature dependence of thermal conductivity and its dependence on the microstructural characteristics.

**References**

1. M. R. Nyden, G. P. Forney, and J. E. Brown, "Molecular modeling of polymer flammability – Application to the design of flame-resistant polyethylene," Macromolecules, 25 (1992), 1658-1666.

2. S. M. Lomakin et al., "An investigation of the thermal-stability and char-forming tendency of cross-linked poly (methyl methacrylate)," Polymer Degradation and Stability, 41 (1993), 229-243.

3. T. Petersen et al., "Microstructure of an industrial char by diffraction techniques and reverse Monte Carlo modeling," Carbon, 42 (2004), 2457-2469.

4. T. Kashiwagi et al., "Nanoparticle network reduce the flammability of polymer nanocomposites," Nature Materials, 4 (2005) 928 -933.

5. T. Kashiwagi et al., "Thermal degradation and flammability properties of poly(propylene)/carbon nanotube composites," Macromolecular Rapid Communications, 23 (2002), 761-765.

6. T. Kashiwagi et al., "Thermal and flammability properties of polypropylene/carbon nanotube composites," Polymer, 45 (2004), 4227-4239.

7. J. C. Phillips, "Topology of covalent non-crystalline solids I: Short-range order in chalcogenide alloys," Journal of Non-Crystalline Solids, 34 (1979), 153-181.

8. M. F. Thorpe, "Continuous deformation in random networks," Journal of Non-Crystalline Solids, 57 (1983), 355-370.

9. J. W. Lawson and D. Srivastava, "Formation and structure of amorphous carbon char from polymer materials," Physical Review B, 77 (2008), 144209.

10. D. W. Brenner, "Empirical potential for hydrocarbons for use in simulating the chemical vapor-deposition of diamond films," Physical Review B, 42 (1990), 9458-9471.

11. H. He and M. F. Thorpe, "Elastic properties of glasses," Physical Review Letters, 54 (1985), 2107-2110.

12. P. Jund and R. Jullien, "Molecular-dynamics calculation of the thermal conductivity of vitreous silica," Physical Review B, 59 (1999), 13707-13711.

13. D. G. Cahill, S. K. Watson, and R. O. Pohl, "Lower limit to the thermal-conductivity of disordered crystals," Physical Review B, 46 (1992), 6131-6140.
(1992)

14. A. J. Bullen et al., "Thermal conductivity of amorphous carbon thin films," Journal of Applied Physics, 88 (2000), 6317-6320.